Received: 17 September 2019 | Revised: 28 February 2020 | Accepted: 29 February 2020

DOI: 10.1111/jace.17092

Journal of the American Ceramic Society

ORIGINAL ARTICLE

Structure, infrared spectra and microwave dielectric properties of the novel Eu_2TiO_5 ceramics

Zheng Jinjie[1] | **Yang Yaokang**[1] | **Wu Haitao**[1] | **Yuanyuan Zhou**[1] | **Zhiliang Zhang**[2]

[1]School of Materials Science and Engineering, University of Jinan, Jinan, PR China

[2]State Key Laboratory of Biobased Material and Green Papermaking, Qilu University of Technology (Shandong Academy of Sciences), Jinan, PR China

Correspondence
Wu Haitao, School of Materials Science and Engineering, University of Jinan, Jinan 250022, PR China.
Email: mse_wuht@ujn.edu.cn

Zhiliang Zhang, State Key Laboratory of Biobased Material and Green Papermaking, Qilu University of Technology (Shandong Academy of Sciences), Jinan 250353, PR China.
Email: zhzhl@iccas.ac.cn

Funding information
National Natural Science Foundation, Grant/Award Number: 51972143; Project funded by China Postdoctoral Science Foundation, Grant/Award Number: 2017M612341

Abstract

The microwave dielectric properties of Eu_2TiO_5 ceramic prepared by a conventional solid-state method were investigated for the first time. An orthorhombic structure with Pnam space group was obtained from x-ray diffraction. On the basis of P-V-L chemical bond theory and refined lattice parameters, the bond parameters of bond ionicity, lattice energy, bond energy, and coefficient of thermal expansion of Eu_2TiO_5 were computed. The relationship between chemical bond characteristics and microwave dielectric properties was discussed. Besides, far-infrared reflective spectra indicated the absorption of structural phonon oscillation might be the main contribution to polarization for Eu_2TiO_5 ceramic. Eu_2TiO_5 ceramic sintered at 1300°C for 6 hours possessed excellent microwave dielectric properties of $\varepsilon_r \sim 14.4 \pm 0.2$, $Q \times f \sim 21\,000 \pm 500$ GHz, and $\tau_f \sim -10 \pm 2$ ppm/°C.

KEYWORDS

Eu_2TiO_5, far-infrared spectrum, microwave dielectric ceramics, P-V-L chemical bond theory

1 | INTRODUCTION

The high frequency extension of TE mode microwave dielectrics materials have attracted more and more research attention due to an increasing demand for filters, dielectric resonator antennas, etc.[1-3] The properties of a low dielectric constant (ε_r), a high quality factor ($Q \times f$), and a near-zero temperature coefficient of resonant (τ_f) are required for microwave dielectric ceramics.[4-6] In recent years, numerous novel microwave dielectric ceramics have been reported, such as $Mg_{2.5}VMoO_8$, $Eu_2Zr_3(MoO_4)_9$, $Li_7Ti_3O_9F$, $CaLa_4Si_3O_{13}$, and Li_4WO_5.[7-13] However, to meet the needs of rapidly developing 5G (fifth-generation wireless systems) and IoT (Internet of Things), the novel dielectric ceramic material with low loss still needs to be investigated.

The AO-Ln_2O_3-TiO_2 system (Ln = rare earth element) microwave dielectric ceramics have been reported to possess high permittivity and excellent properties.[14,15] For instance, Okawa et al reported that $BaLa_4Ti_4O_{15}$ microwave dielectric ceramic exhibited properties of $\varepsilon_r = 46$, $Q \times f = 46\,000$ GHz, $\tau_f = -11$ ppm/°C.[14] Subsequently, Tohdo et al prepared $ALa_4Ti_4O_{15}$ (A = Ba, Sr, and Ca) dielectric properties ceramics and the properties were reported.[15] But there is few research on the Ln_2O_3-TiO_2 dielectric ceramics system. Li et al reported the $La_4Ti_3O_{12}$ and $Eu_4Ti_3O_{12}$ fabricated by the sol-gel method possessed usable properties of $\varepsilon_r = 19.68$, $Q \times f = 9950$ GHz, $\tau_f = -9.95$ ppm/°C and $\varepsilon_r = 27.51$, $Q \times f = 9450$ GHz, $\tau_f = 211$ ppm/°C, respectively.[16,17] Particularly, two phases of Eu_2TiO_5 and $Eu_2Ti_2O_7$ were found in sintered $Eu_4Ti_3O_{12}$ samples. However, the microwave

dielectric properties of pure phase Eu_2TiO_5 have not been investigated. Furthermore, the P-V-L chemical bond theory has been used to study the intrinsic factors of dielectric properties. For example, Yang et al calculated the bond characteristics of $NdNbO_4$ with $(Zr_{0.5}W_{0.5})^{5+}$ ion substitution and reported the Nb-site covalency, lattice energy, and bond energy were closely related to microwave dielectric properties.[18] Zhang et al reported that the dielectric constant, quality factor, and temperature coefficient of resonant of $La_2(Zr_{1-x}Ti_x)_3(MoO_4)_9$ were in good agreement with bond iconicity, lattice energy, and thermal expansion coefficient as a variation of Ti^{4+} substitution, respectively.[19] Besides, the P-V-L theory was also used for Y_2MgTiO_6, $Mg_2(Ti_{1-x}Sn_x)O_4$, $Gd_2Zr_3(MoO_4)_9$, etc.[20-24] It was meaningful to calculate the chemical bond parameters of Eu_2TiO_5 ceramic using P-V-L theory.

In this work, the pure-phase Eu_2TiO_5 ceramic was prepared by the conventional solid-state method. The phase composition, sintering characteristics, microstructure, and microwave dielectric properties were studied. Moreover the intrinsic factors of dielectric properties were investigated via the P-V-L chemical bond theory and far-infrared reflective spectroscopy.

2 | EXPERIMENTAL PROCEDURES

Eu_2TiO_5 ceramics were prepared by the solid-state reaction method using Eu_2O_3 (99.99%, Aladdin, China), and TiO_2 (99.99%, Aladdin, China) powders as the raw material. According to the stoichiometric ratio of Eu_2TiO_5, the start materials were weighted and ball-milled for 24 hours. Then the mixed powder was calcined at 1000°C for 4 hours and reground. After dried, the Eu_2TiO_5 powder was mixed with 8 wt.% paraffin as binder. After that, the powder was pressed into cylinders (about 10 mm in diameter and 6 mm in height). The paraffin was burned out at 500°C for 4 hours. The cylinders were finally sintered at 1200-1400°C for 6 hours with heating and cooling rate of 5°C/min.

The crystal structure and phase composition of the sintered samples were examined by x-ray diffraction with Cu K_α radiation (XRD, D/MAX-B; Rigaku Co.) and the results were identified using ICDD PDF card. The lattice parameter of Eu_2TiO_5 ceramic was performed via Rietveld refinement using FullProf software. Microstructures were analyzed via scanning electron microscopy (SEM, Model JEOL JEM-2010; FEI Co.). Apparent densities were measured by Archimedes method using an analytical balance (XS64; Mettler Toledo). The diametric shrinkage ratio was calculated by Equation (1)

$$\text{Diametric shrinkage ratio} = \frac{D - D_0}{D_0} \times 100\% \quad (1)$$

where D and D_0 are the diameter of sintered sample and green body. The far-infrared reflective spectra were obtained by a Bruker IFS 66v FTIR spectrometer on Infrared beamline station (U4). The ε_r and $Q \times f$ values were measured according to Hakki-Coleman method[25] and cavity method[26] using network analyzer (N5234A; Agilent Co.). τ_f values were calculated by Equation (2).

$$\tau_f = \frac{f_2 - f_1}{f_1 (85 - 25)} \quad (2)$$

where f_1 and f_2 are the resonant frequency at 25 and 85°C, respectively.

3 | RESULTS AND DISCUSSION

Figure 1 shows the XRD patterns of Eu_2TiO_5 powders calcined at 1000°C and ceramics sintered at 1200°C-1400°C. For powders calcined at 1000°C, it was clear that all the diffraction peaks were index to Eu_2TiO_5 (PDF#01-82-1009), indicating a pure Eu_2TiO_5 phase could be synthesis at 1000°C. The similar results were gained for patterns of sintered samples. With no second phase detected, an orthorhombic structure with space group of Pnam (62) could be obtained at the sintering temperature of 1200°C-1400°C.

To further explore the crystal structure of Eu_2TiO_5 ceramic, Rietveld refinement was conducted and the results are presented in Figure 2A. The lattice constant of Eu_2TiO_5 was refined as $a = 10.5342(5)$ Å, $b = 11.2957(5)$ Å, $c = 3.7785(6)$ Å, $\alpha = \beta = \gamma = 90.0000°$, and $V = 449.61(4)$ Å^3 with orthorhombic structure (space group Pnam). The reliability factors R_p, R_{wp}, as well as R_{exp} of 2.25%, 2.87%, and 2.52% were gained, which indicated calculated patterns showed a great agreement

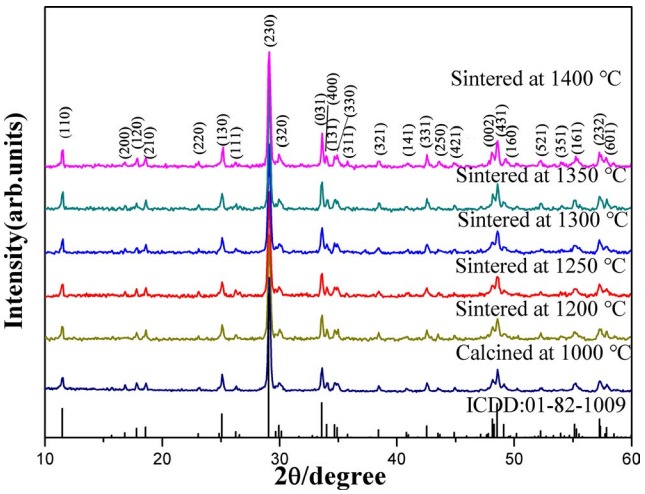

FIGURE 1 XRD patterns of Eu_2TiO_5 calcined at 1000°C and ceramics sintered at 1200-1400°C [Color figure can be viewed at wileyonlinelibrary.com]

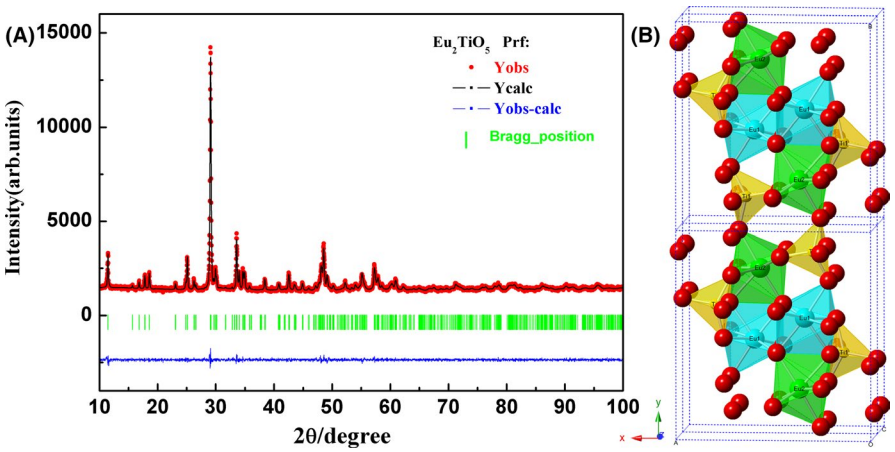

FIGURE 2 (A) Rietveld refinement patterns of Eu_2TiO_5 ceramic sintered at 1300°C, (B) schematic diagram of the crystal structure for Eu_2TiO_5 ceramic [Color figure can be viewed at wileyonlinelibrary.com]

on the observed patterns. According to the refined lattice parameters, the Wyckoff position, coordinates and occupancy were listed in the Table 1. The schematic diagram of the crystal structure for Eu_2TiO_5 was revealed in Figure 2B. There were two possible Eu-sits (Eu(1), Eu(2)), only one set of Ti-sites and five sets of O-sits (O(1)-O(5)). All ions occupy the 4c Wyckoff positions, the Eu^{3+} are coordinated with seven oxygen anions while Ti^{4+} are coordinated with five oxygen anions.

Figure 3 showed the SEM images of the surface of Eu_2TiO_5 ceramics sintered at 1200°C-1400°C. As shown in Figure 3A,B, porous microstructure was observed for ceramics sintered at 1200°C and 1250°C, which may result in lower apparent density and damaging dielectric properties. As we all know, grain growth is an important factor for densification during the sintering process.[27] The grain sizes gradually increased with the increasing of temperature, which showed positive correlation with sintering temperatures. It was evident that Eu_2TiO_5 sintered at 1300°C exhibited a relatively dense microstructure with fewer pores, indicating that nearly compact was obtained. However, micro-crack was observed above 1300°C shown in Figure 3E, which might degenerate the density and quality factor.[28]

The diametric shrinkage rate and apparent density of Eu_2TiO_5 ceramics at different sintering temperature were presented in Figure 4. The diametric shrinkage rate increased with sintering temperature until 1300°C due to the grain growth, while the apparent density increased to a maximum of 6.09 g/cm^3. With the further increase of sintering temperatures, density exhibited a slight downward trend, which can be attributed to the presence of micro-crack as shown in Figure 3E. The decrease in shrinkage rate was related to ceramics deformation at 1400°C. The Eu_2TiO_5 sintered at 1300°C possessed 95.5% of theoretical density, which was consistent with the results of SEM.

Figure 5 presents ε_r, $Q \times f$, and τ_f of Eu_2TiO_5 ceramics as a function of sintering temperatures. The variation in ε_r was similar to that of apparent density with sintering temperatures. The dielectric constant increased firstly, reaching a maximum value at 1300°C, and then showed a slight decrease with further increasing sintering temperature. To analyze the influence of porosity on the ε_r, relative permittivity corrected for porosity was calculated using Bosman and Havinga method (Equation 3).[29]

$$\varepsilon_{\text{corr.}} = \varepsilon_m (1 + 1.5p) \tag{3}$$

where the $\varepsilon_{\text{corr.}}$, ε_m, and p are corrected permittivity, measured permittivity, and fractional porosity, respectively. For

TABLE 1 Atomic coordinates of the Eu_2TiO_5

Atomic	Site	*x/a*	*y/b*	*z/c*	Occupancy
Eu(1)	4c	0.1372 (3)	0.0593 (3)	0.25000	0.50000
Eu(2)	4c	0.3911 (3)	0.2209 (3)	0.75000	0.50000
Ti(1)	4c	0.1803 (8)	0.3790 (11)	0.25000	0.50000
O(1)	4c	0.008 (3)	0.108 (3)	0.75000	0.50000
O(2)	4c	0.281 (3)	0.039 (3)	0.75000	0.50000
O(3)	4c	0.233 (3)	0.386 (3)	0.75000	0.50000
O(4)	4c	0.260 (3)	0.239 (2)	0.25000	0.50000
O(5)	4c	0.010 (3)	0.350 (3)	0.25000	0.50000

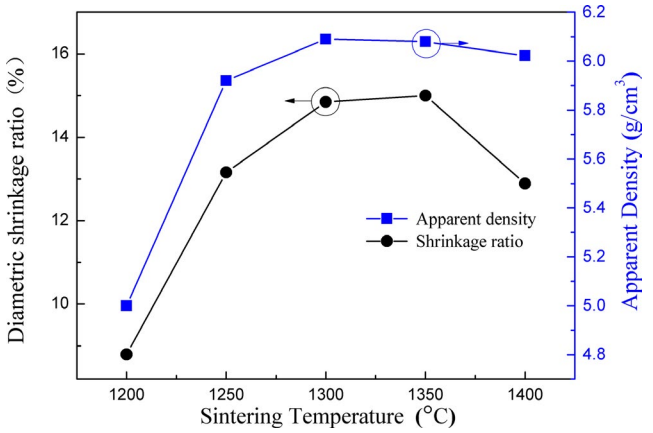

FIGURE 3 Apparent density and diametric shrinkage ratio of Eu_2TiO_5 ceramics sintered from 1200 to 1400°C [Color figure can be viewed at wileyonlinelibrary.com]

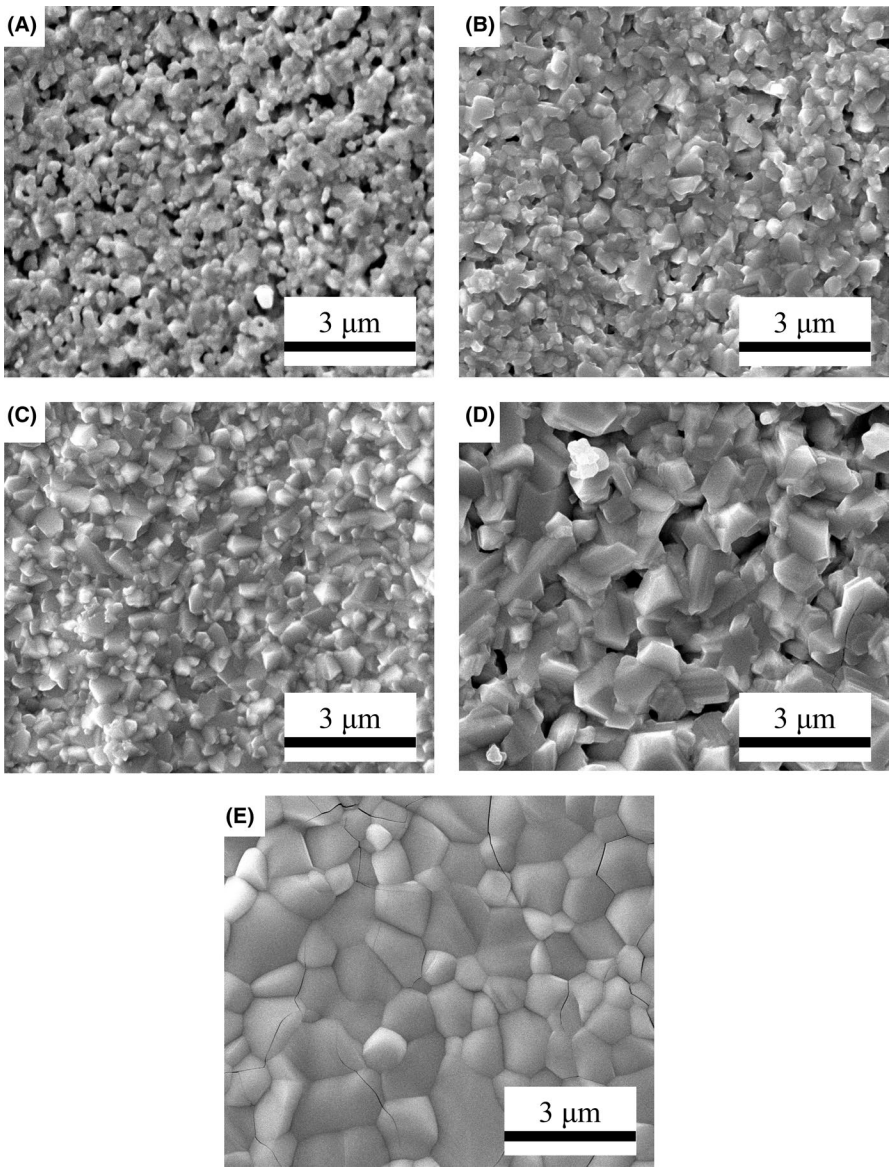

FIGURE 4 SEM images of Eu_2TiO_5 ceramics sintered at (A) 1200°C, (B) 1250°C, (C) 1300°C, (D) 1350°C, (E) 1400°C

Eu_2TiO_5 ceramic sintered at 1300°C, the maximum ε_m of 14.4 accompanied by relative density of 95.5% were obtained. Accordingly, the ε_{corr} of Eu_2TiO_5 sintered at 1300°C was calculated to be 15.35. Except for extrinsic factors such as compactness, second phase, and porosity, the ε_r is also affected by intrinsic factors like polarizability. The total polarizability(α) of Eu_2TiO_5 could be calculated as follows:

$$\alpha(Eu_2TiO_5) = 2\alpha(Eu^{3+}) + \alpha(Ti^{4+}) + 5\alpha(O^{2-}) \quad (4)$$

where the $\alpha(Eu^{3+})$, $\alpha(Ti^{4+})$, and $\alpha(O^{2-})$ are the ionic polarizability values of Eu^{3+}, Ti^{4+}, and O^{2-}, respectively.[30] In addition, the theoretical dielectric constant ($\varepsilon_{thero.}$) was calculated according to Clausius-Mossotti equation, as expressed in Equation (5).

$$\varepsilon_{thero.} = \frac{3V_m + 8\pi\alpha}{3V_m - 4\pi\alpha} \quad (5)$$

In the equation, V_m and α are the mole volume of the primitive cell and polarizability of Eu_2TiO_5, respectively. The theoretical permittivity (14.79) of the Eu_2TiO_5 ceramic is close to the corrected permittivity (15.35).

The $Q \times f$ values showed a similar tendency to density and ε_r, suggesting that the density was the domination factor in Eu_2TiO_5 ceramics. Eu_2TiO_5 ceramic sintered at 1300°C possessed the optimum $Q \times f$ value of 21 000 GHz. When the sintering temperatures increased to 1350°C, a significant downward trend was observed, which might be ascribed to micro-crack at high temperature shown in SEM images.[28] The τ_f exhibited a slight decrease from −7.8 to −17.4 ppm/°C with increasing sintering temperature. As a result, the optimal microwave dielectric properties with ε_r of 14.4 ± 0.2, $Q \times f$ of 21 000 ± 500 GHz, and τ_f of −10 ± 2 ppm/°C were gained for Eu_2TiO_5 ceramic at 1300°C. In order to compare this work with other materials, 273 microwave dielectric materials with dielectric constant

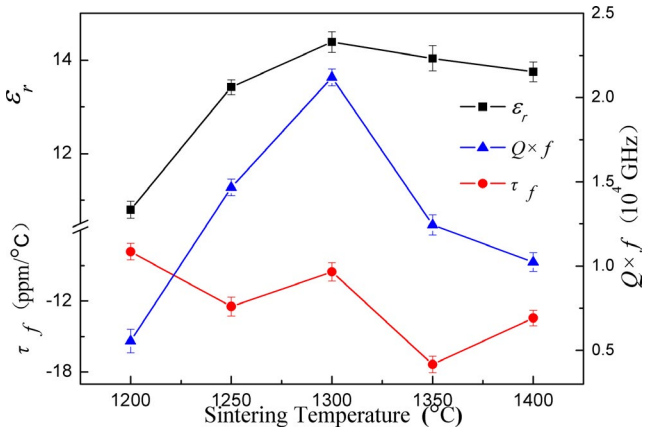

FIGURE 5 Microwave dielectric properties of Eu_2TiO_5 ceramics at different sintering temperature [Color figure can be viewed at wileyonlinelibrary.com]

of 12 to 16 were chosen, in which the date is come from *Low-loss dielectric ceramic materials and their properties* reported by MT Sebastian.[31] As shown in Figure 6, the quality factor of Eu_2TiO_5 ceramic is higher than approximately 36% of material with similar dielectric constant, but far below the optimal materials like $(Mg_{0.95}Zn_{0.05})_4Ta_2O_9$.[32] The quality factor seems lower now and if for the practical application, the ceramics should be modified to improve the Qf values in further work. The τ_f value is better than about 70% of materials with similar dielectric constant.

Phillips, Van Vechten, and Levine first reported the relationship between chemical bond parameters and dielectric properties.[33-35] Then the chemical bond theory was applied to complex crystal through splitting the multiple compounds into binary crystals by Zhang.[36] It was proved that chemical bond parameters computed according P-V-L chemical bond theory were the critical intrinsic factors for microwave dielectric properties.[37-39] According to the atoms information and coordinated condition show in Table 1 and Figure 2B, the binary expressions of Eu_2TiO_5 could be written as follows:

$$\begin{aligned} Eu_2TiO_5 = {} & Eu(1)_{3/7}O(1)_{3/4} + Eu(1)_{2/7}O(2)_{1/2} + Eu(1)_{1/7}O(3)_{1/4} \\ & + Eu(1)_{1/7}O(4)_{1/4} + Eu(2)_{1/7}O(1)_{1/4} + Eu(2)_{1/7}O(2)_{1/4} \\ & + Eu(2)_{1/7}O(3)_{1/4} + Eu(2)_{2/7}O(4)_{1/2} + Eu(2)_{2/7}O(5)_{2/3} \\ & + Ti_{1/5}O(2)_{1/4} + Ti_{2/5}O(3)_{1/2} + Ti_{1/5}O(4)_{1/4} + Ti_{1/5}O(5)_{1/3} \end{aligned} \quad (6)$$

On the basis of the refined lattice constant, chemical bond theory and our previous works,[8,19] the chemical bond parameters of bond ionicity (*fi*), lattice energy (*U*), bond energy (*E*), and the coefficient of thermal expansion (α) were calculated. The results were exhibited in Table 2, while the average values were illustrated in Figure 7. As shown in Figure 7, the *fi*(Eu(1)-O), *fi* (Eu(2)-O), and *fi* (Ti-O) of 0.8817, 0.8599, and 0.7704 were obtained, respectively. The

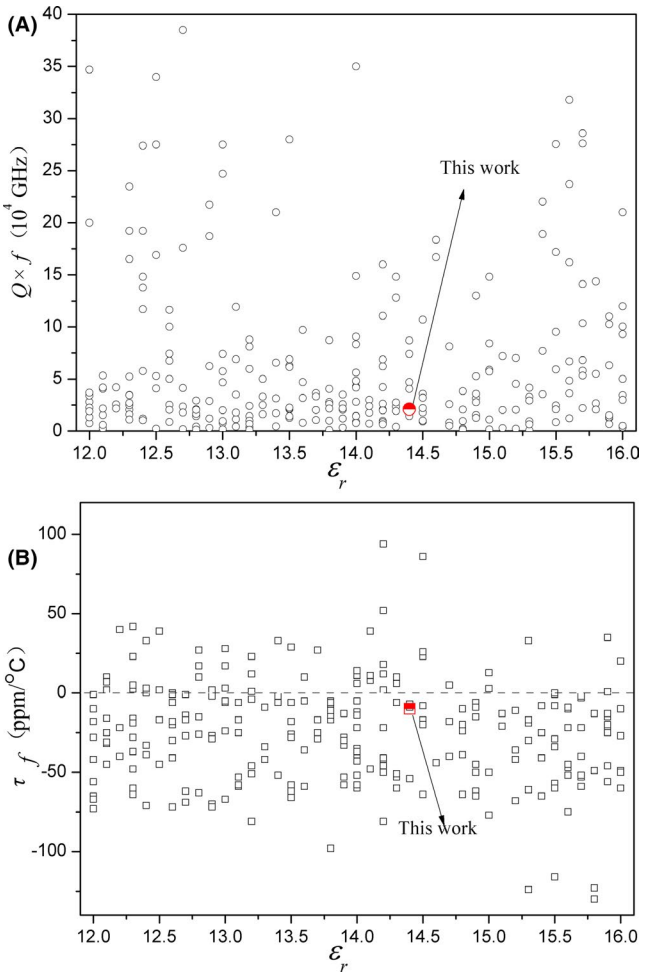

FIGURE 6 Relationship between quality factor (A), temperature coefficient of resonant (B) and dielectric constant [Color figure can be viewed at wileyonlinelibrary.com]

dielectric constant was positively correlated with the bond iconicity, which the relationship is shown as Equation (7).

$$\varepsilon_r = \frac{n^2-1}{1-f_i} + 1 \quad (7)$$

where the *n* is refractive index. Therefore, the *fi*(Eu(1)-O) make biggest contribution to the ε_r of Eu_2TiO_5 ceramics. It was reported that the lattice energy and bond energy were associated with the $Q \times f$ and τ_f values, respectively.[37,40] The same sequence of U(Ti-O)>U(Eu(2)-O)>U(Eu(1)-O) and E(Ti-O)>E(Eu(2)-O)>E(Eu(1)-O) were obtained, indicating the Ti-O bond is the most important factors of $Q \times f$ and τ_f values. In addition, the τ_f can be calculated as follows:

$$\tau_f = -\frac{\tau_\varepsilon}{2} - \alpha \quad (8)$$

where the τ_ε is the temperature coefficient of the relative permittivity and the α is the thermal expansion coefficient.

Bond type	Bond length (Å)	f_i	E (kJ/mol)	U (kJ/mol)	α (10^{-6} K^{-1})
Eu1-O1[1] × 2	2.3926	0.8815	307.4520	1799	7.3112
Eu1-O1[2]	2.4312	0.8821	302.5707	888	7.4469
Eu1-O2 × 2	2.4324	0.8821	302.4214	1775	7.4529
Eu1-O3	2.3878	0.8814	308.0701	900	7.3054
Eu1-O4	2.4070	0.8817	305.6127	895	7.3639
Eu2-O1	2.2917	0.8797	320.9887	930	6.9675
Eu2-O2	2.3594	0.8809	311.7783	910	7.1903
Eu2-O3	2.5003	0.8830	294.2086	868	7.6915
Eu2-O4 × 2	2.3491	0.8807	313.1454	1825	7.1619
Eu2-O5 × 2	2.4041	0.7753	305.9814	1677	7.0516
Ti-O2	1.8527	0.8028	414.9989	2992	2.6056
Ti-O3 × 2	1.9707	0.8066	390.1499	5721	2.8711
Ti-O4	1.7904	0.8003	429.4395	3065	2.4681
Ti-O5	1.8236	0.6720	421.6212	2724	2.4690
Eu1-$O_{avg.}$		0.8817	305.2254	1251.4	7.3760
Eu2-$O_{avg.}$		0.8599	309.2205	1242.0	7.2125
Ti-$O_{avg.}$		0.7704	414.0524	3625.5	2.6034

TABLE 2 Bond ionicity (*fi*), lattice energy (*U*), bond energy (*E*), and the coefficient of thermal expansion (α) of each bond for Eu_2TiO_5 ceramics

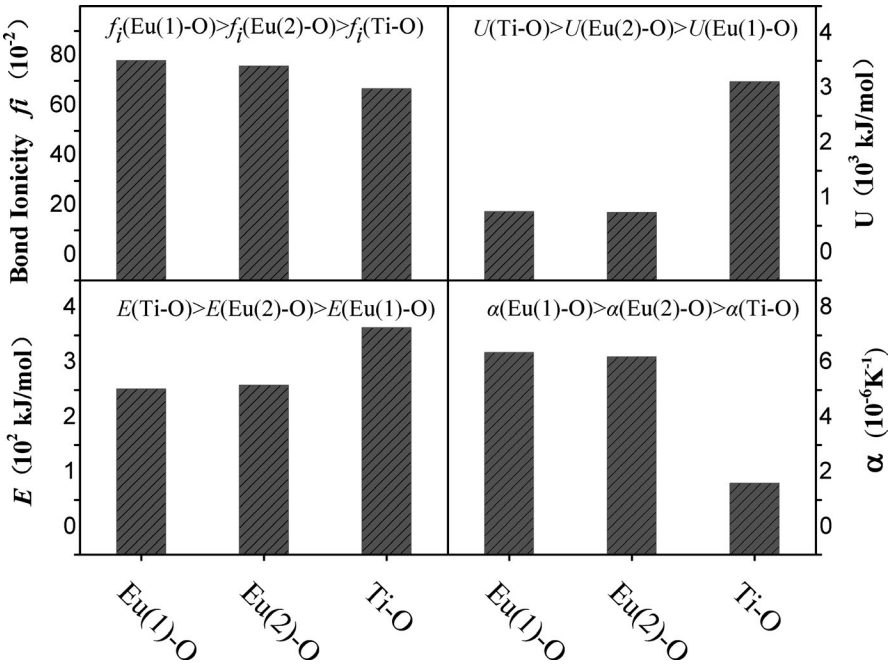

FIGURE 7 Bond iconicity (*fi*), lattice energy (*U*), bond energy (*E*), and the coefficient of thermal expansion (α) of Eu_2TiO_5 ceramic

Consequently, the smaller the α, the smaller the values of τ_f. It can be observed that the value of α(Ti-O) is smaller than that of Eu(2)-O and Eu(1)-O bond, which indicated α(Ti-O) play the major role in Eu_2TiO_5 ceramics.

The far-infrared reflective spectrum was carried out to characterize the intrinsic dielectric properties of Eu_2TiO_5 ceramics, the measured and fitted IR reflectivity spectra were illustrated in Figure 8A. The IR reflectivity spectra can be well fitted using 21 resonant modes tabulated in Table 3. According to Drude-Lorentz model, the complex dielectric function $\varepsilon(\omega)$ and complex reflectivity $R(\omega)$ can be expressed as follows[41,42]:

$$\varepsilon^*(\omega) = \varepsilon_\infty + \sum_{j=1}^{n} \frac{\omega_{pj}^2}{\omega_{oj^2} - \omega^2 - j\gamma_j - j\gamma_j\omega} \tag{9}$$

$$R(\omega) = \left| \frac{1 - \sqrt{\varepsilon^*(\omega)}}{1 + \sqrt{\varepsilon^*(\omega)}} \right|^2 \tag{10}$$

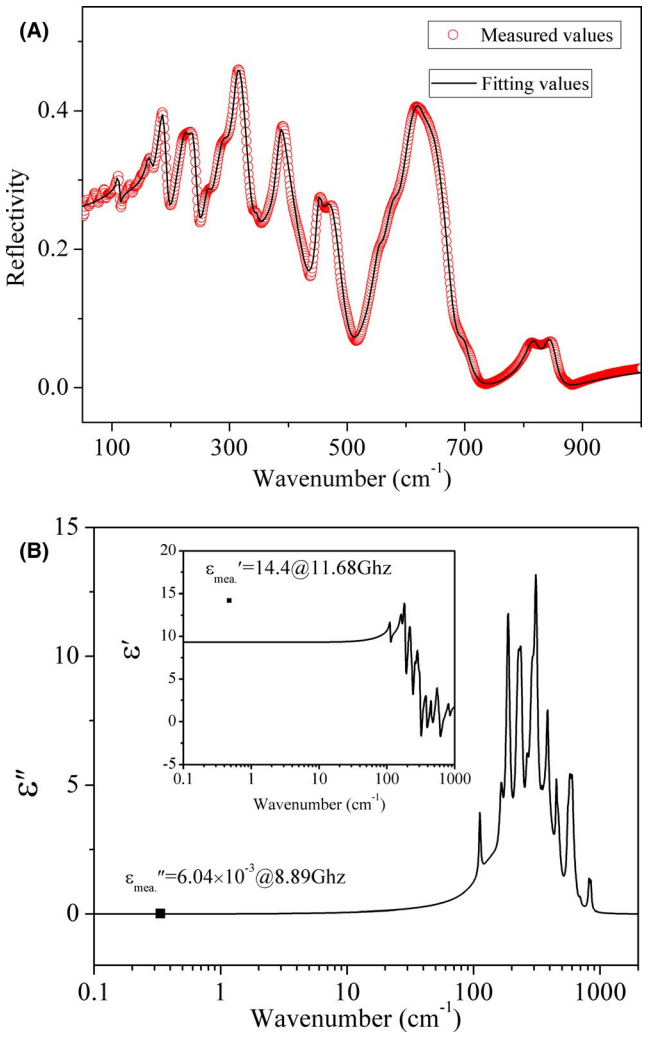

FIGURE 8 A, Measured and fitted infrared reflectivity spectra of Eu_2TiO_5 ceramic sintered at 1300°C. B, Real and imaginary parts of complex permittivity for Eu_2TiO_5 ceramic [Color figure can be viewed at wileyonlinelibrary.com]

Figure 8B depicted the imaginary and real parts of the permittivity. A smaller calculated dielectric constant (9.3) compared to measurements (14.4) was gained as seen from Figure 8B. Due to the higher eigenfrequencies at FIR range than the measured microwave frequency, some polarizations at lower frequency may be neglected in far-infrared spectrum, which might result in the lower real parts of the permittivity.[43] Besides, the calculated dielectric loss exhibited a same order of magnitude with measured loss, implying that the majority of microwave dielectric loss is dominant by the absorptions of structural phonon oscillation at the infrared region.

4 | CONCLUSIONS

In this work, Eu_2TiO_5 ceramics were prepared through the solid-state reaction. The XRD and Rietveld refinement showed a pure orthorhombic phase with space group of Pnam (62) at 1200-1400°C. Besides, the intrinsic dielectric properties were investigated by P-V-L chemical bond theory and far-infrared reflective spectroscopy. The ε_r was mainly attributed to the iconicity of Eu–O bond, while the $Q \times f$ was closely related to the lattice energy and bond energy of Ti–O bond. The coefficient of thermal expansion of Ti–O bond was important factor of τ_f for Eu_2TiO_5 ceramic. The far-infrared reflective spectrum indicated that the majority polarization contribution is dominant by the absorptions of structural phonon oscillation at the infrared region. Excellent microwave dielectric properties of $\varepsilon_r = 14.4 \pm 0.2$, $Q \times f = 21\,000 \pm 500$ GHz, and $\tau_f = -10 \pm 2$ ppm/°C were gained for Eu_2TiO_5 ceramic sintered at 1300°C for 6 hours.

TABLE 3 Phonon parameters obtained from the fitting of the far-infrared spectra of Eu_2TiO_5 ceramics

Modes	ω_{oj}	ω_{pj}	γ_j	$\Delta_{\varepsilon j}$
1	112.08	32.79	4.00	0.0855
2	143.67	139.96	89.04	0.9489
3	165.36	66.99	11.38	0.1641
4	187.03	160.13	14.23	0.7330
5	225.16	192.08	23.21	0.7277
6	237.27	134.24	15.16	0.3201
7	636.01	100.24	42.61	0.0248
8	553.87	136.51	20.62	0.0607
9	263.94	97.65	16.40	0.1369
10	289.38	229.88	29.78	0.6311
11	310.96	247.02	21.56	0.6311
12	344.92	23.01	5.52	0.0044
13	378.87	401.15	105.38	1.1211
14	383.80	148.00	17.19	0.1487
15	450.28	101.48	11.46	0.0508
16	465.03	208.43	39.07	0.2009
17	574.14	243.96	33.09	0.1806
18	600.44	310.06	40.53	0.2667
19	694.95	66.79	26.28	0.0092
20	816.57	160.08	29.55	0.0384
21	842.39	146.42	26.60	0.0302
$\varepsilon_\infty = 2.7906$				

ACKNOWLEDGMENT

This work was supported by the National Natural Science Foundation (no. 51972143) and Project funded by China Postdoctoral Science Foundation (2017M612341). The authors thank Professor Zeming Qi and Chuansheng Hu in IR beamline workstation of National Synchrotron Radiation Laboratory (NSRL) for the IR measurement.

ORCID

Wu Haitao https://orcid.org/0000-0002-9106-8574

REFERENCES

1. Zhou D, Pang LX, Wang DW, Li C, Jin BB, Reaney IM. High permittivity and low loss microwave dielectrics suitable for 5G resonators and low temperature co-fired ceramic architecture. J Mater Chem C. 2017;5:10094–8.
2. Yongduk O, Bharambe V, Mummareddy B, Martin J, McKnight J, Abraham MA, et al. Microwave dielectric properties of zirconia fabricated using NanoParticle Jetting™. Addit Manuf. 2019;27:586–94.
3. Reaney IM, Iddles D. Microwave dielectric ceramics for resonators and filters in mobile phone networks. J Am Ceram Soc. 2006;89(7):2063–72.
4. Sebastian MT, Jantunen H. Low loss dielectric materials for LTCC applications: a review. Int Mate Rev. 2008;53(2):57–90.
5. Manan A, Ullah Z, Ahmad AS, Ullah A, Khan DF, Hussain A, et al. Phase microstructure evaluation and microwave dielectric properties of $(1–x)Mg_{0.95}N_{i0.05}Ti_{0.98}Zr_{0.02}O_3$-$xCa_{0.6}La_{0.8/3}TiO_3$ ceramics. J Adv Ceram. 2018;7(1):72–8.
6. Sebastian MT, Ubic R, Jantunen H, editors. Microwave materials and applications. Hoboken: John Wiley & Sons, 2017.
7. Naveenraj R, Arun NS, Ratheesh R. Structure and microwave dielectric properties of low-temperature sinterable $A_{2.5}VMoO_8$ (A = Mg, Zn) molybdovanadate ceramics. Appl Phys A. 2020;126(53):1–8.
8. Zhang YH, Sun JJ, Dai N, Wu ZC, Wu HT, Yang CH. Crystal structure, infrared spectra and microwave dielectric properties of novel extra low-temperature fired $Eu_2Zr_3(MoO_4)_9$ ceramics. J Eur Ceram Soc. 2019;39(4):1127–31.
9. Zhang Z, Fang L, Xiang H, Xu M, Tang Y, Jantunen H, et al. Structural, infrared reflectivity spectra and microwave dielectric properties of the $Li_7Ti_3O_9F$ ceramic. Ceram Int. 2019;45(8):10163–9.
10. Song J, Song K, Wei J, Lin H, Xu J, Wu J, et al. Microstructure characteristics and microwave dielectric properties of calcium apatite ceramics as microwave substrates. J Alloys Compd. 2018;731(15):264–70.
11. Li J, Fang L, Luo H, Khaliq J, Tang Y, Li CC. Li_4WO_5: a temperature stable low-firing microwave dielectric ceramic with rock salt structure. J Eur Ceram Soc. 2016;36(1):243–6.
12. Xiang HC, Fang L, Fang WS, Tang Y, Li CC. A novel low-firing microwave dielectric ceramic $Li_2ZnGe_3O_8$ with cubic spinel structure. J Eur Ceram Soc. 2017;37(2):625–9.
13. Li CC, Xiang HC, Xu MY, Tang Y, Fang L. Li_2AGeO_4 (A=Zn, Mg): two novel low-permittivity microwave dielectric ceramics with olivine structure. J Eur Ceram Soc. 2018;38(4):1524–8.
14. Okawa T, Kiuchi K, Okabe H, Ohsato H. Microwave dielectric properties of $Ba_nLa_4Ti_{3+n}O_{12+3n}$ homologous series. Jpn J Appl Phys. 2001;40(9S):5779–82.
15. Tohdo Y, Kakimoto K, Ohsato H, Yamada H, Okawa T. Microwave dielectric properties and crystal structure of homologous compounds $ALa_4Ti_4O_{15}$ (A = Ba, Sr and Ca) for base station applications. J Eur Ceram Soc. 2006;26(10–11):2039–43.
16. Li ZF, Wu WJ, Liu F, Li YX, Si PZ, Ge HL. Microwave dielectric properties of $La_4Ti_3O_{12}$ ceramics. Mater Lett. 2014;118:24–6.
17. Li ZF, Li DP, Wu WJ, Liu F, Li YX, Si PZ, et al. Microwave dielectric properties of $Eu_4Ti_3O_{12}$ ceramics via Sol-Gel method. Adv Mater Res. 2013;750:1020–3.
18. Yang HC, Zhang SR, Yang HY, Yuan Y, Li EZ. Bond characteristics, vibrational spectrum and optimized microwave dielectric properties of chemically substituted $NdNbO_4$. Ceram Int. 2019;45(14):16940–7.
19. Zhang YH, Wu HT. Crystal structure and microwave dielectric properties of $La_2(Zr_{1-x}Ti_x)_3(MoO_4)_9$ ($0 \le x \le 01$) ceramics. J Am Ceram Soc. 2019;102(7):4092–102.
20. Yang HC, Zhang SR, Yang HY, Yuan Y, Li EZ. Vibrational spectroscopic and crystal chemical analyses of double perovskite Y_2MgTiO_6 microwave dielectric ceramics. J Am Ceram Soc. 2020;103(2):1121–30.
21. Li H, Zhang PC, Yu SQ, Yang HY, Tang B, Li FH, et al. Structural dependence of microwave dielectric properties of spinel structured $Mg_2(Ti_{1-x}Sn_x)O_4$ solid solutions: crystal structure refinement, Raman spectra study and complex chemical bond theory. Ceram Int. 2019;45(9):11639–47.
22. Xing CF, Wu B, Bao J, Wu HT, Zhou YY. Crystal structure, infrared spectra and microwave dielectric properties of a novel low-fring $Gd_2Zr_3(MoO_4)_9$ ceramic. Ceram Int. 2019;45(17):22207–14.
23. Xiao M, Wei YS, Zhang P. The correlations between complex chemical bond theory and microwave dielectric properties of $Ca_2MgSi_2O_7$ ceramics. J Electron Mater. 2019;48(3):1652–9.
24. Zhang P, Wu SX, Xiao M. The microwave dielectric properties and crystal structure of low temperature sintering $LiNiPO_4$ ceramics. J Eur Ceram Soc. 2018;38(13):4433–9.
25. Hakki BW, Coleman PD. A dielectric resonator method of measuring inductive capacities in the millimeter range. IEEE Trans Microwave Theory Tech. 1960;8(4):402–10.
26. Courtney WE. Analysis and evaluation of a method of measuring the complex permittivity and permeability microwave insulators. IEEE Trans Microwave Theory Tech. 1970;18(8):476–85.
27. Xiang HC, Bai Y, Li CC, Fang L, Jantunen HL. Structural, thermal and microwave dielectric properties of the novel microwave material $Ba_2TiGe_2O_8$. Ceram Int. 2018;44(9):10824–8.
28. Jaakola T, Möttönen J, Uusimäki A, Rautioaho R, Leppävuori S. Preparation of Nd-doped $Ba_2Ti_9O_{20}$ ceramics for use in microwave applications. Ceram Int. 1987;13(3):151–7.
29. Bosman AJ, Havinga EE. Temperature dependence of dielectric constants of cubic ionic compounds. Phys Rev. 1963;129(4):1593–600.
30. Shannon RD. Dielectric polarizabilities of ions in oxides and fluorides. J Appl Phys. 1993;73(1):348–66.
31. Sebastian MT, Ubic R, Jantunen H. Low-loss dielectric ceramic materials and their properties. Int Mater Rev. 2015;60(7):392–412.
32. Huang CL, Chu CH, Liu FS, Yu PC. High Q microwave dielectrics in the $(Mg_{1-x}Zn_x)_4Ta_2O_5$ ceramics. J Alloys Compd. 2014;590:494–9.
33. Phillips JC. Ionicity of the chemical bond in crystals. Rev Mod Phys. 1970;42(3):317–56.
34. Van Vechten JA. Quantum dielectric theory of electronegativity in covalent systems II Ionization potentials and interband transition energies. Phys Rev. 1969;187(3):1007–20.
35. Levine BF. Bond susceptibilities and ionicities in complex crystal structures. J Chem Phys. 1973;59(3):1463–86.
36. Xue D, Zhang S. Calculation of the nonlinear optical coefficient of the $NdAl_3(BO_3)_4$ crystal. J Phys-Condens Mat. 1996;8(12):1949–56.
37. Xiao M, Sun HR, Zhou ZQ, Zhang P. Bond ionicity, lattice energy, bond energy, and microwave dielectric properties of $Ca_{1-x}Sr_xWO_4$ ceramics. Ceram Int. 2018;44(17):20686–91.

38. Xia WS, Li LX, Ning PF, Liao QW. Relationship between bond ionicity, lattice energy, and microwave dielectric properties of $Zn(Ta_{1-x}Nb_x)_2O_6$ ceramics. J Am Ceram Soc. 2012;95(8):2587–92.
39. Bi JX, Xing CF, Yang CH, Wu HT. Phase composition, microstructure and microwave dielectric properties of rock salt structured Li_2ZrO_3-MgO ceramics. J Eur Ceram Soc. 2018;38(11):3840–6.
40. Xiao M, He SS, Lou J, Zhang P. Structure and microwave dielectric properties of $MgZr(Nb_{1-x}Sb_x)_2O_8$ ($0 \le x \le 01$) ceramics. J Alloys Compd. 2019;777:350–7.
41. Pang LX, Zhou D. Modification of $NdNbO_4$ microwave dielectric ceramic by Bi substitutions. J Am Ceram Soc. 2019;102(5):2278–82.
42. Guo HH, Zhou D, Pang LX, Qi ZM. Microwave dielectric properties of low firing temperature stable scheelite structured (Ca, Bi)(Mo, V)O_4 solid solution ceramics for LTCC applications. J Eur Ceram Soc. 2019;39(7):2365–73.
43. Yang Y, Wang Y, Zheng J, Dai N, Li R, Wu H, et al. Microwave dielectric properties of ultra-low loss $Li_2Mg_4Zr_{0.95}(Mg_{1/3}Ta_{2/3})_{0.05}O_7$ ceramics sintered at low temperature by LiF addition. J Alloys Compd. 2019;786:867–72.

How to cite this article: Jinjie Z, Yaokang Y, Haitao W, Zhou Y, Zhang Z. Structure, infrared spectra and microwave dielectric properties of the novel Eu_2TiO_5 ceramics. *J Am Ceram Soc*. 2020;103:4333–4341. https://doi.org/10.1111/jace.17092